Protein Engineering

International Edition: DOI: 10.1002/anie.201903455
German Edition: DOI: 10.1002/ange.201903455

Biocatalytic Strategy for Highly Diastereo- and Enantioselective Synthesis of 2,3-Dihydrobenzofuran-Based Tricyclic Scaffolds

David A. Vargas, Rahul L. Khade, Yong Zhang, and Rudi Fasan**

Abstract: *2,3-Dihydrobenzofurans are key pharmacophores in many natural and synthetic bioactive molecules. A biocatalytic strategy is reported here for the highly diastereo- and enantioselective construction of stereochemically rich 2,3-dihydrobenzofurans in high enantiopurity (>99.9% de and ee), high yields, and on a preparative scale via benzofuran cyclopropanation with engineered myoglobins. Computational and structure-reactivity studies provide insights into the mechanism of this reaction, enabling the elaboration of a stereochemical model that can rationalize the high stereoselectivity of the biocatalyst. This information was leveraged to implement a highly stereoselective route to a drug molecule and a tricyclic scaffold featuring five stereogenic centers via a single-enzyme transformation. This work expands the biocatalytic toolbox for asymmetric C–C bond transformations and should prove useful for further development of metalloprotein catalysts for abiotic carbene transfer reactions.*

Benzofuran and 2,3-dihydrobenzofuran scaffolds are key structural motifs and pharmacophores in many bioactive natural products and synthetic compounds (Figure 1).[1] Methods for the synthesis and elaboration of these scaffolds

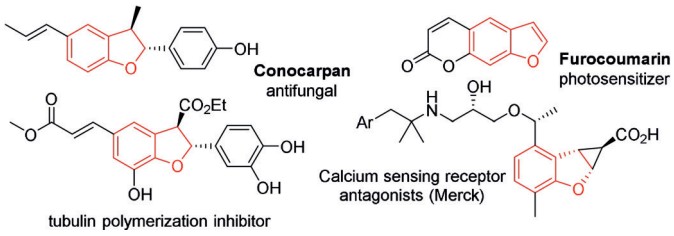

Figure 1. Biologically active molecules containing 2,3-dihydrobenzofuran and benzofuran moieties.

are therefore of significant interest in organic and medicinal chemistry.[1] The metal-catalyzed cyclopropanation of benzofurans with diazo reagents provides an attractive strategy for the preparation of 2,3-dihydrobenzofurans.[2] While important advances in asymmetric benzofuran cyclopropanations have been made using Rh-based catalysts in the presence of donor–acceptor diazo reagents,[2,3] the stereoselective cyclopropanation of benzofurans using readily available and inexpensive acceptor-only diazoester reagents has proven very challenging.[1d,e,4] Furthermore, iron-based (bio)catalysts useful for promoting metallo-carbenoid cyclopropanations of benzofurans have thus far remained elusive.

Engineered heme-containing proteins have recently emerged as promising biocatalysts for mediating selective carbene transfer reactions, including olefin cyclopropanation,[5] Y–H insertion (where Y = N, S, or Si),[6] C–H functionalization,[7] aldehyde olefination,[8] and other relevant transformations.[9] In particular, our group has previously reported the high activity and selectivity of engineered variants of sperm whale myoglobin (Mb) for promoting asymmetric olefin cyclopropanations in the presence of acceptor-only diazo reagents, including α-diazoacetates,[5c,d] 2-diazotrifluoroethane,[10] and diazoacetonitrile.[11] Building upon these findings and motivated by the shortcomings of current methodologies in the context of carbene-mediated transformations as outlined above, we report here the development of a Mb-based biocatalytic strategy for the highly diastereo- and enantioselective cyclopropanation of benzofurans with an acceptor-only carbene donor. This strategy provides a new, efficient, and highly stereoselective route to afford 2,3-dihydrobenzofuran scaffolds of high value for medicinal chemistry and drug synthesis.

Initial tests with wild-type myoglobin (Mb), its distal histidine variant Mb(H64V), and a panel of other hemoproteins (for example, P450s, cyt *c*, and horseradish peroxidase) showed no activity in the desired cyclopropanation of benzofuran (**1**) with ethyl α-diazoacetate (**2a**, Supporting Information, Table S9). Using Mb(H64V) as background, we then tested a mini-library of Mb variants in which the shape of the heme pocket is systematically varied by substituting each of the amino acid residues within this cavity (i.e., Leu29, Phe43, Val68, and Ile107) with an apolar amino acid of significantly different size (for example, Leu29 was mutated to Ala or Phe; Phe43 was mutated to Ile or Ser). Promisingly, this strategy led to the successful identification of Mb(H64V,V68A)[5c] as a viable catalyst for converting **1** to the desired product **3a**. Notably, neither Fe(TPP) nor hemin can catalyze this reaction, highlighting the critical role of the protein matrix in conferring benzofuran cyclopropanation reactivity to the protein-embedded iron-porphyrin. Despite its modest catalytic activity (19% conversion; Table 1, Entry 3), Mb(H64V,V68A) was determined to exhibit excellent diastereo- and enantioselectivity (>99.9% *de* and *ee*) in

[*] D. A. Vargas, Prof. Dr. R. Fasan
Department of Chemistry, University of Rochester
120 Trustee Road, Rochester, NY 14627 (USA)
E-mail: rfasan@ur.rochester.edu
Dr. R. L. Khade, Prof. Dr. Y. Zhang
Department of Chemistry and Chemical Biology,
Stevens Institute of Technology, Hoboken, NJ 07030 (USA)
E-mail: yong.zhang@stevens.edu
Supporting information and the ORCID identification number(s) for the author(s) of this article can be found under:
https://doi.org/10.1002/anie.201903455.

Table 1: Activity and selectivity of myoglobin variant in the cyclopropanation of benzofuran with EDA and other diazoesters.[a]

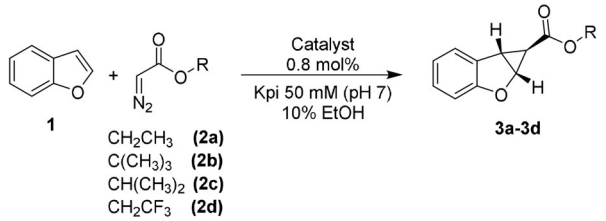

Entry	Catalyst	diazo	Equiv 2a–d/ *T*	Yield[b] (TON)	% *de*	% *ee*
1	hemin	**2a**	1/RT	0	–	–
2	Mb	**2a**	1/RT	0	–	–
3	Mb(H64V,V68A)	**2a**	1/RT	19% (24)	>99	>99
4	Mb(H64A,V68A)	**2a**	1/RT	29% (36)	>99	>99
5	Mb(H64G,V68A)	**2a**	1/RT	39% (49)	>99	>99
6	Mb(H64G,V68A)	**2a**	2/RT	45% (56)	>99	>99
7[c]	Mb(H64G,V68A)	**2a**	2/RT	76% (95)	>99	>99
8[c]	Mb(H64G,V68A)	**2a**	2/3 °C	>99% (125)	>99	>99
9[c]	Mb(H64G,V68A)	**2b**	2/3 °C	13% (16)	>99	>99
10[c]	Mb(H64G,V68A)	**2c**	2/3 °C	36% (45)	>99	>99
11[c]	Mb(H64G,V68A)	**2d**	2/3 °C	>99% (125)	>99	>99
12[c,d]	Mb(H64G,V68A)	**2a**	2/3 °C	89% (445)	>99	>99
13[c]	Mb(H64G,V68A) (*E. coli* cells)[e]	**2a**	2/3 °C	78% (59)	>99	>99

[a] Conditions: 20 μM catalyst, 2.5 mM benzofuran, 2.5 or 5 mM diazo compound, 10 mM $Na_2S_2O_4$, 16 h, anaerobic conditions. [b] GC yield. [c] Slow diazo addition. [d] 5 μM protein. [e] $OD_{600}=50$.

this reaction producing the (1*R*,1a*R*,6b*S*)-configured isomer (see below) as the only detectable product. Based on the previously established importance of the gating Val64 residue in controlling access of the olefin substrate to the heme pocket in Mb(H64V,V68A)-catalyzed cyclopropanation of styrene,[12] the crucial V68A mutation (Supporting Information, Table S9) was then combined with smaller residues at position 64 (i.e., Ala, Gly), in an effort to increase catalytic activity by favoring access of the larger benzofuran substrate to the heme-carbene intermediate. Gratifyingly, the corresponding variants Mb(H64A,V68A) and Mb(H64G,V68A) showed a progressive improvement in catalytic activity, while maintaining excellent stereoselectivity (>99.9% *de* and *ee*; Table 1, Entries 4–5).

Using Mb(H64G,V68A), further improvements in both the catalytic turnovers (TON) and product conversions were then obtained via optimization of pH, EDA:benzofuran ratio, and temperature (Supporting Information, Table S10). Under optimal conditions, full conversion of benzofuran to enantiopure **3a** was achieved using 0.8 mol% of Mb(H64G,V68A) (Table 1, Entry 8). Various other diazo esters (**2b–d**) are compatible with this reaction, furnishing **3b–d** with excellent levels of stereoselectivity (>99.9% *de* and *ee*; Table 1, Entries 9–11), albeit in reduced yields in the case of the bulkier diazo reagents **3b** and **3c**. With EDA, high product conversion (89%) was obtained also with a 4-fold lower catalyst loading (0.2 mol%), corresponding to a TON of 445 (Table 1, Entry 12). Moreover, comparable yields of **3a** were achieved using *Escherichia coli* expressing Mb(H64G,V68A) (Table 1, Entry 13), thus demonstrating the possibility to perform this biocatalytic transformation using whole cells. While offering excellent enantioselectivity and involving an iron-based biocatalyst, the *trans*-selectivity of Mb(H64G,V68A) nicely complements the *cis*-selectivity of a Ir-salen catalyst previously reported by Katsuki and coworkers for a related transformation.[4a]

Encouraged by these results, we further investigated the substrate scope of the Mb(H64G,V68A) biocatalyst using various substituted benzofurans (Scheme 1). Substitution on the benzofuran molecule with both electron-donating and electron-withdrawing groups were well tolerated by the biocatalyst, enabling the highly diastereo- and enantioselective (>99.9% *de* and *ee*) synthesis of the corresponding tricyclic products **5a–c**, **5e–i** with good to quantitative conversion (61–99%; Scheme 1). Bulkier substrates, such as the

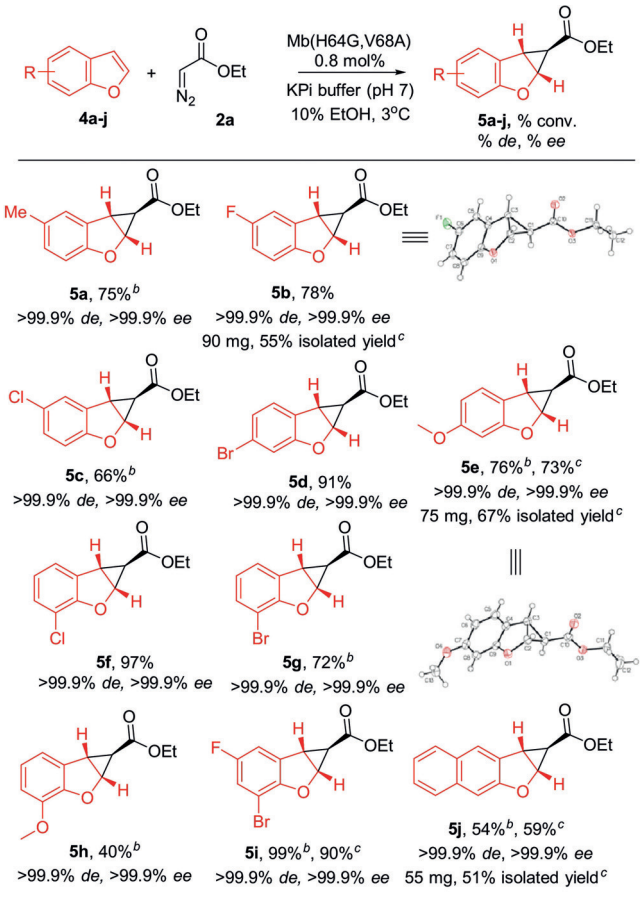

Scheme 1. Substrate scope for Mb(H64G,V68A)-catalyzed cyclopropanation of benzofurans with EDA.[a] [a] As in Table 1 Entry 8. [b] 15 mM EDA. [c] Using whole-cells ($OD_{600}=50$).

disubstituted derivative **4i** and naphtho[2,3-b]furan (**4j**), could be also efficiently processed by the Mb-based carbene transferase to give **5i** and **5j** in enantiopure form. Comparable results were observed for whole-cell biotransformations using Mb(H64G,V68A)-expressing cells (for example, 90% yield and >99% *de* and *ee* for **5i**). Furthermore, the Mb(H64G,V68A)-catalyzed reaction with representative substrates such as 5-fluoro- (**4b**), naphtho[2,3-b]furan (**4j**), and 6-methoxy-benzofuran (**4e**) could be readily performed on a preparative scale to afford 55–90 mg of the corresponding cyclopropanation products in 55% (**5b**), 51% (**5j**), and 67% (**5e**) isolated yield. Crystallographic analysis of **5b**, **5d**, and **5f** (Supporting Information, Figures S2–4), and chiral chromatography analysis of the other products (Supporting Information, Table S7), indicated that the Mb(H64G,V68A) exhibits a remarkably conserved stereoselectivity toward formation of the *exo* (1*R*,1a*R*,6b*S*)-configured tricyclic product. This combination of exquisite stereocontrol and broad substrate scope has little precedent in the context of new-to-nature enzyme-catalyzed reactions.[13]

Interestingly, both Mb(H64V,V68A) and Mb(H64G,V68A) exhibit a divergent chemoselectivity in the reaction with benzofuran vs. the structurally related indole, the latter leading exclusively to the C(3)-H functionalization product.[7c] Both reactions can occur (or compete) with these heterocycles in the presence of other catalytic systems[14] (for Rh: see Figure S6 in the Supporting Information). To gain insights into the mechanism of the present reaction and the basis for this divergent chemoselectivity, both transformations were investigated via Density Functional Theory (DFT) using a model of histidine-ligated Fe–porphyrin (see the Supporting Information for details). In each case, both a mechanism involving a direct C_2=C_3 carbene insertion ("ins") and one proceeding via a zwitterionic ("zw") intermediate were considered (Figure 2). For the indole reaction, a direct carbene C–H insertion was ruled out based on isotope labeling experiments conducted with both Mb(H64V, V68A)[7c] and Mb(H64G,V68A) (Supporting Information, Figure S5). For both reaction pathways, the calculated transition state (TS) geometries with benzofuran vs. indole are similar. Consistent with a nucleophilic attack through the C3 position of the heterocycle, the TS structures for the stepwise pathway shows a shorter distance (approximately 0.3 Å) between the C3 atom and the carbene C1 carbon atom compared to the C2···C1 distance (2.19 vs. 2.48 Å for benzofuran and 2.36 vs. 2.67 Å for indole; Figure 2). In both $TS_{O/zw}$ and $TS_{N/zw}$, the plane of the heterocycle is perpendicular to the carbene ester group, projecting the C2–H and C3–H bonds toward the porphyrin ring. In comparison, the TS structures for the C_2=C_3 insertion pathway show a significantly different orientation of the heterocycle ring with respect to the carbene group (Figure 2). Moreover, the C2 atom is now closer to the carbene C1 compared to the C3 atom (C2···C1(2.22/2.30 Å) < C3···C1(2.52/2.38 Å) for benzofuran/indole; Figure 2). Despite these similarities, the relative energy of TS_{ins} vs. TS_{zw} differ significantly between the two heterocycles. For indole, $TS_{N/zw}$ is indeed 1.5 kcal mol^{-1} lower in energy than $TS_{N/ins}$ ($\Delta G^{\ddagger}$ = 6.8 vs. 8.3 kcal mol^{-1}; Figure 2), indicating that C(3)-H functionalization by the heme-carbene is favored over cyclopropanation with this substrate.[15] In contrast, the energy barriers for the two pathways in the benzofuran

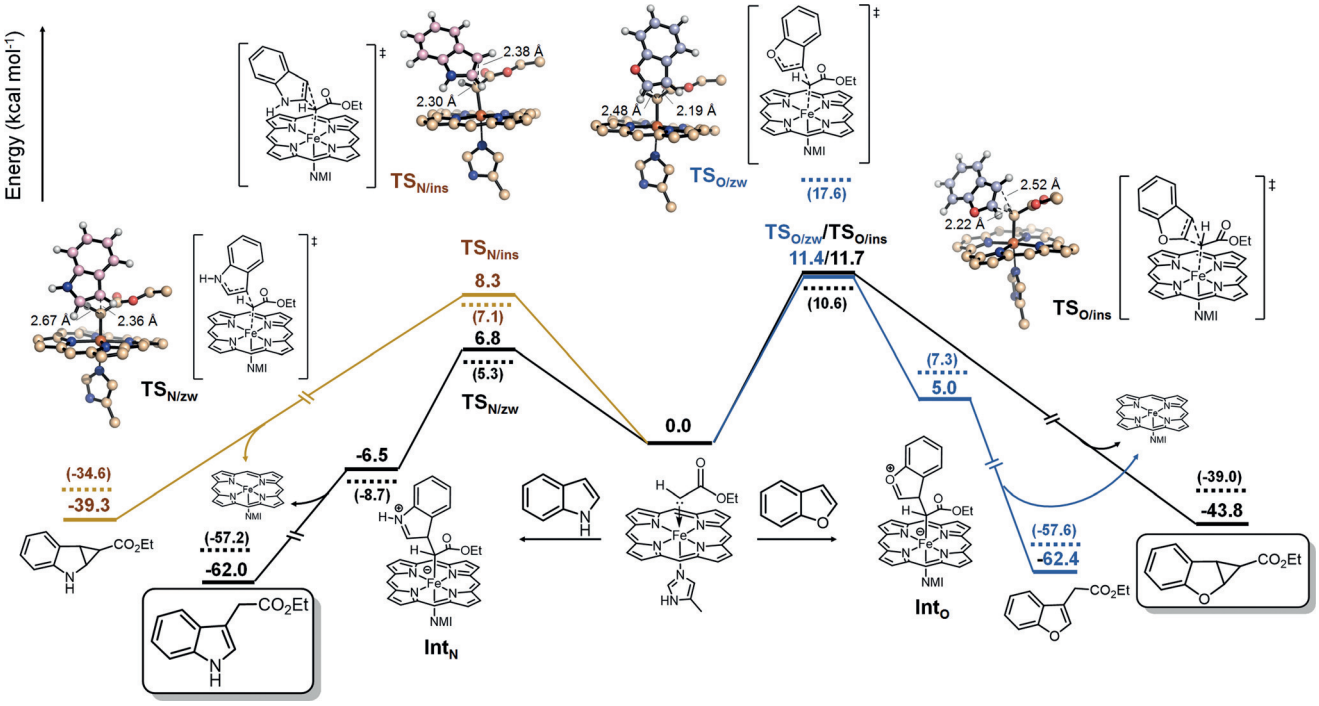

Figure 2. Gibbs free energy diagram for the heme-carbene reactions with benzofuran and indole. ΔG values calculated at the ωB97XD/6–311G(d)-LANL2DZ level (see the Supporting Information for details). NMI = 5-methyl-imidazole. Dotted bars and values in brackets correspond to transition states (TS) in the protein active site model (see the Supporting Information for details).

reaction are comparable ($\Delta G^{\ddagger} = 11.4$–$11.7$ kcal mol^{-1} ($TS_{O/ins}$); Figure 2). However, when the active site residues surrounding the heme-carbene are included in the calculations (see the Supporting Information for details), the C_2=C_3 insertion step becomes significantly more favorable ($\Delta G^{\ddagger} =$ 10.6 ($TS_{O/ins}$) vs. 17.6 kcal mol^{-1} ($TS_{O/zw}$); Figure 2), suggesting a key role of the protein matrix in favoring this reaction. To further discriminate which process is operative in the metalloprotein, we reasoned that the two pathways should be differentially impacted by substitution at the level of the C2 and C3 position of benzofuran, as given by the differential steric constraints around these sites in the corresponding TS structures (Figure 2). Experimentally, Mb(H64G,V68A) was found to show significant cyclopropanation activity on 3-methyl-benzofuran, but no activity on 2-methyl-benzofuran (Scheme 2). These results are consistent with the C_2=C_3

R_1	R_2	Yield	TON
H	H	56%	139
CH_3	H	7%	4
H	CH_3	0%	0

R_1	R_2	Yield	TON
H	H	99%	250
CH_3	H	0%	0
H	CH_3	10%	24

Scheme 2. Reactivity studies with 2- and 3-methyl benzofurans.

insertion mechanism, as this is expected to be significantly more tolerant to steric encumbrance at the C3 vs. the C2 site compared to the stepwise mechanism. These conclusions are further corroborated by the results with 2-methyl-indole, which can be converted by the enzyme with modest but measurable activity (Scheme 2). Since $TS_{O/zw}$ and $TS_{N/zw}$ have similar geometries (Figure 2), the distinct reactivity trend observed with the 2-substitued heterocycles further supports a mechanistic scenario whereby benzofuran cyclopropanation proceeds via a concerted, asymmetric carbene insertion with nucleophilic attack to the carbene initiating from the C2 end of the C_2=C_3 bond (i.e., via $TS_{O/ins}$).

Based on these results, $TS_{O/ins}$ was docked into the structure of Mb(H64G,V68A), as modeled based on the crystal structure of Mb(H64V,V68A).[12] In the resulting complex (Figure 3), which is consistent with the stereochemical outcome of the cyclopropanation reaction, the carbene ester group extends into an inner cavity between Ala68 and Ile107, whereas the benzofuran molecule approaches the heme-bound carbene via an opening created by the Gly residue at position 64. This arrangement enforces attack of the heterocycle in *trans* with respect to the carbene-borne ester group and to the *si* face of the carbene group (the *re* face being shielded by Phe43; Figure 3), thereby explaining the absolute diastereo- and enantioselectivity of the biocatalyst in this reaction. This model is also consistent with the beneficial effect of the large-to-small mutations in position 64 (His ≪ Val < Ala < Gly; Table 1), as these should facilitate access of the benzofuran to heme-bound carbene through the solvent-exposed side of the heme group (ring C/D), and the tolerance of the biocatalyst to substitutions on the aromatic ring of

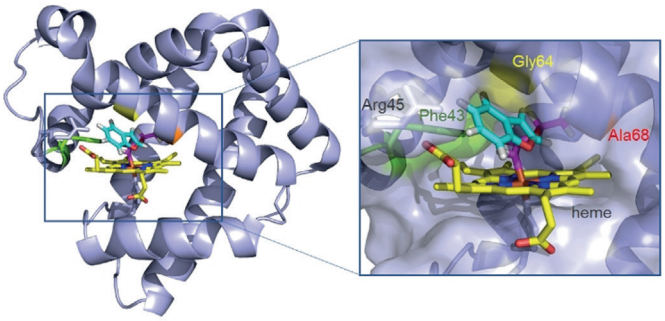

Figure 3. Model of $TS_{O/ins}$ complex (cyan/purple) in Mb(H64G,V68A) structure.

benzofuran, as suggested by the available space surrounding these positions, especially at positions 6 and 7, which are solvent-exposed (Figure 3).

Leveraging these insights, a double, Mb(H64G,V68A)-catalyzed asymmetric cyclopropanation was accomplished using 7-vinyl-benzofuran (**4k**) to give **5k** in high enantiopurity (>99.9% *de* and *ee*; Scheme 3a). Time-course experiments

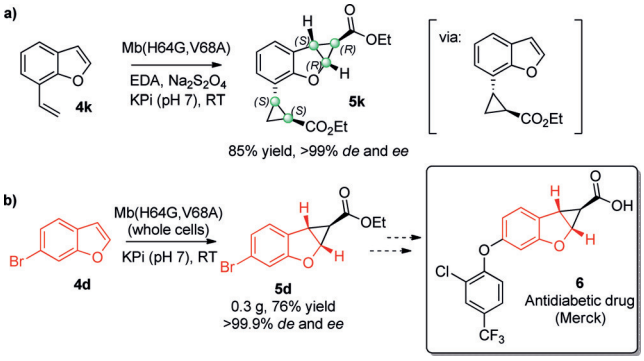

Scheme 3. Mb(H64G,V68A)-catalyzed stereoselective synthesis of **5k** and antidiabetic drug **6**.

confirmed that cyclopropanation of vinyl group occurs first, followed by C_2=C_3 cyclopropanation. Notably, this transformation enables the creation of five stereogenic centers with high stereoselectivity using a single enzyme. Finally, Mb(H64G,V68A) could be applied to access 0.3 g of the tricyclic compound **5d** in 76% isolated yield and enantiopure form as a potential precursor for a highly stereoselective synthesis of Merck's antidiabetic drug **6** (Scheme 3b). Of note, the latter was previously prepared as a mixture of stereoisomers, requiring the isolation of the desired enantiomer by chiral phase chromatography.[1d]

In conclusion, we reported here the first example of a biocatalytic (and iron-based) strategy for asymmetric benzofuran cyclopropanation to afford stereochemically rich 2,3-dihydrobenzofuran scaffolds of high value for medicinal chemistry. In addition to excellent stereoselectivity, this method offers good substrate scope, scalability, and compatibility with whole-cell biotransformations. Our studies yielded valuable insights into the mechanism of this reaction that helped elucidate metalloprotein-mediated stereoinduction

and informed the application of this methodology to enable the highly enantioselective synthesis of a drug precursor and a sterochemically rich tricyclic scaffold bearing five stereogenic centers via a single-enzyme transformation. The present findings expand the biocatalytic toolbox for abiotic reactions[13] and should aid the further development of metalloprotein catalysts for selective carbene transfer reactions.

Acknowledgements

This work was supported by the U.S. National Institute of Health grant GM098628 (R.F) and a National Science Foundation grant CHE-1300912 (Y.Z). D.V. acknowledges support from the NSF Graduate Fellowship Program. The authors are grateful to Dr. William Brennessel for assistance with crystallographic analyses and Noah Gubernick for technical assistance. MS and X-ray instrumentation are supported by U.S. National Science Foundation grants CHE-0946653 and CHE-1725028.

Conflict of interest

The authors declare no conflict of interest.

Keywords: benzofuran cyclopropanation · biocatalysis · carbene transfer · dihydrobenzofurans · myoglobin

How to cite: *Angew. Chem. Int. Ed.* **2019**, *58*, 10148–10152
Angew. Chem. **2019**, *131*, 10254–10258

[1] a) R. J. Nevagi, S. N. Dighe, S. N. Dighe, *Eur. J. Med. Chem.* **2015**, *97*, 561–581; b) L. N. Qin, D. D. Vo, A. Nakhai, C. D. Andersson, M. Elofsson, *ACS Comb. Sci.* **2017**, *19*, 370–376; c) M. M. Heravi, V. Zadsirjan, H. Hamidi, P. H. T. Amiri, *RSC Adv.* **2017**, *7*, 24470–24521; d) M. Ge, J. He, F. Wai, G.-B. Liang, S. Lin, W. Liu, S. P. Walsh, L. Yang (Merk and Co.), US2007/0265332A1, **2007**; e) C. Zhou, S. Wang, G. Zhang (Beigene, Ltd.), **2013**.

[2] a) S. J. Hedley, D. L. Ventura, P. M. Dominiak, C. L. Nygren, H. M. L. Davies, *J. Org. Chem.* **2006**, *71*, 5349–5356; b) H. M. L. Davies, S. J. Hedley, *Chem. Soc. Rev.* **2007**, *36*, 1109–1119.

[3] a) A. DeAngelis, O. Dmitrenko, G. P. A. Yap, J. M. Fox, *J. Am. Chem. Soc.* **2009**, *131*, 7230–7231; b) V. Lehner, H. M. L. Davies, O. Reiser, *Org. Lett.* **2017**, *19*, 4722–4725.

[4] a) H. Suematsu, S. Kanchiku, T. Uchida, T. Katsuki, *J. Am. Chem. Soc.* **2008**, *130*, 10327–10337; b) M. L. Rosenberg, K. Vlasana, N. Sen Gupta, D. Wragg, M. Tilset, *J. Org. Chem.* **2011**, *76*, 2465–2470.

[5] a) P. S. Coelho, E. M. Brustad, A. Kannan, F. H. Arnold, *Science* **2013**, *339*, 307–310; b) P. S. Coelho, Z. J. Wang, M. E. Ener, S. A. Baril, A. Kannan, F. H. Arnold, E. M. Brustad, *Nat. Chem. Biol.* **2013**, *9*, 485–487; c) M. Bordeaux, V. Tyagi, R. Fasan, *Angew. Chem. Int. Ed.* **2015**, *54*, 1744–1748; *Angew. Chem.* **2015**, *127*, 1764–1768; d) P. Bajaj, G. Sreenilayam, V. Tyagi, R. Fasan, *Angew. Chem. Int. Ed.* **2016**, *55*, 16110–16114; *Angew. Chem.* **2016**, *128*, 16344–16348; e) J. G. Gober, A. E. Rydeen, E. J. Gibson-O'Grady, J. B. Leuthaeuser, J. S. Fetrow, E. M. Brustad, *ChemBioChem* **2016**, *17*, 394–397; f) K. Oohora, H. Meichin, L. M. Zhao, M. W. Wolf, A. Nakayama, J. Hasegawa, N. Lehnert, T. Hayashi, *J. Am. Chem. Soc.* **2017**, *139*, 17265–17268; g) A. M. Knight, S. B. J. Kan, R. D. Lewis, O. F. Brandenberg, K. Chen, F. H. Arnold, *ACS Cent. Sci.* **2018**, *4*, 372–377; h) E. J. Moore, V. Steck, P. Bajaj, R. Fasan, *J. Org. Chem.* **2018**, *83*, 7480–7490; i) O. F. Brandenberg, C. K. Prier, K. Chen, A. M. Knight, Z. Wu, F. H. Arnold, *ACS Catal.* **2018**, *8*, 2629–2634.

[6] a) Z. J. Wang, N. E. Peck, H. Renata, F. H. Arnold, *Chem. Sci.* **2014**, *5*, 598–601; b) G. Sreenilayam, R. Fasan, *Chem. Commun.* **2015**, *51*, 1532–1534; c) V. Tyagi, R. B. Bonn, R. Fasan, *Chem. Sci.* **2015**, *6*, 2488–2494; d) S. B. J. Kan, R. D. Lewis, K. Chen, F. H. Arnold, *Science* **2016**, *354*, 1048–1051; e) M. W. Wolf, D. A. Vargas, N. Lehnert, *Inorg. Chem.* **2017**, *56*, 5623–5635.

[7] a) P. Dydio, H. M. Key, A. Nazarenko, J. Y. Rha, V. Seyedkazemi, D. S. Clark, J. F. Hartwig, *Science* **2016**, *354*, 102–106; b) G. Sreenilayam, E. J. Moore, V. Steck, R. Fasan, *Adv. Synth. Catal.* **2017**, *359*, 2076–2089; c) D. A. Vargas, A. Tinoco, V. Tyagi, R. Fasan, *Angew. Chem. Int. Ed.* **2018**, *57*, 9911–9915; *Angew. Chem.* **2018**, *130*, 10059–10063.

[8] a) V. Tyagi, R. Fasan, *Angew. Chem. Int. Ed.* **2016**, *55*, 2512–2516; *Angew. Chem.* **2016**, *128*, 2558–2562; b) M. J. Weissenborn, S. A. Low, N. Borlinghaus, M. Kuhn, S. Kummer, F. Rami, B. Plietker, B. Hauer, *ChemCatChem* **2016**, *8*, 1636–1640.

[9] a) V. Tyagi, G. Sreenilayam, P. Bajaj, A. Tinoco, R. Fasan, *Angew. Chem. Int. Ed.* **2016**, *55*, 13562–13566; *Angew. Chem.* **2016**, *128*, 13760–13764; b) K. Chen, X. Y. Huang, S. B. J. Kan, R. K. Zhang, F. H. Arnold, *Science* **2018**, *360*, 71–75.

[10] A. Tinoco, V. Steck, V. Tyagi, R. Fasan, *J. Am. Chem. Soc.* **2017**, *139*, 5293–5296.

[11] A. L. Chandgude, R. Fasan, *Angew. Chem. Int. Ed.* **2018**, *57*, 15852–15856; *Angew. Chem.* **2018**, *130*, 16078–16082.

[12] A. Tinoco, Y. Wei, J.-P. Bacik, D. M. Carminati, E. J. Moore, N. Ando, Y. Zhang, R. Fasan, *ACS Catal.* **2019**, *9*, 1514–1524.

[13] a) M. T. Reetz, *Top. Organometal. Chem.* **2009**, *25*, 63–92; b) F. Rosati, G. Roelfes, *ChemCatChem* **2010**, *2*, 916–927; c) P. J. Deuss, R. den Heeten, W. Laan, P. C. J. Kamer, *Chem. Eur. J.* **2011**, *17*, 4680–4698; d) H. Renata, Z. J. Wang, F. H. Arnold, *Angew. Chem. Int. Ed.* **2015**, *54*, 3351–3367; *Angew. Chem.* **2015**, *127*, 3408–3426; e) O. F. Brandenberg, R. Fasan, F. H. Arnold, *Curr. Opin. Biotechnol.* **2017**, *47*, 102–111; f) F. Schwizer, Y. Okamoto, T. Heinisch, Y. F. Gu, M. M. Pellizzoni, V. Lebrun, R. Reuter, V. Kohler, J. C. Lewis, T. R. Ward, *Chem. Rev.* **2018**, *118*, 142–231; g) Y. Yu, C. Hu, L. Xia, J. Y. Wang, *ACS Catal.* **2018**, *8*, 1851–1863.

[14] a) G. Özüduru, T. Schubach, M. M. K. Boysen, *Org. Lett.* **2012**, *14*, 4990–4993; b) M. Delgado-Rebollo, A. Prieto, P. J. Perez, *ChemCatChem* **2014**, *6*, 2047–2052; c) Y. Xia, Z. Liu, S. Feng, Y. Zhang, J. B. Wang, *J. Org. Chem.* **2015**, *80*, 223–236.

[15] NMR spectroscopic monitoring of the enzymatic reactions with indole (or N-methyl-indole) and EDA showed no evidence of a cyclopropane precursor to the C3-alkylation product, disfavoring an alternative mechanism involving a cyclopropanation/ring opening pathway as observed in ref. [14b].

Manuscript received: March 20, 2019
Revised manuscript received: May 3, 2019
Accepted manuscript online: May 17, 2019
Version of record online: June 24, 2019

